

# HIGHER ORDER GRADIENT CONTINUUM DESCRIPTION OF ATOMISTIC MODELS FOR CRYSTALLINE SOLIDS

Marcel Arndt\*, Michael Griebel\*

\*Institute for Numerical Simulation, University of Bonn,  
Wegelerstr. 6, 53115 Bonn, Germany  
e-mail: {arndt,griebel}@ins.uni-bonn.de, web page: <http://www.ins.uni-bonn.de>

**Key words:** continuum limit, quasi-continuum approximation, upscaling, molecular dynamics, continuum mechanics, multiscale simulation

**Abstract.** *We propose an upscaling scheme for the passage from atomistic to continuum mechanical models of crystalline solids. It is based on a Taylor expansion of the deformation function up to a given order and describes the material properties to a higher extent than commonly used continuum mechanical models. In particular, the discreteness effects of the underlying atomistic model are captured. The qualitative properties of the technique are numerically analyzed for the model problem of a one-dimensional atomic chain. The approach is then applied to the real three-dimensional physical example of a silicon crystal. The resulting approximation properties are studied in a stationary setting. Finally, a numerical simulation of the time evolution of the elastic response of crystal silicon is presented.*

## 1 INTRODUCTION

The complex behavior of many materials can in general involve quite different length scales. Here, macroscopic effects can often be well described by models on the continuum mechanical level, whereas for microscopical effects on the atomistic level the method of Molecular Dynamics (MD) is appropriate. Sometimes it is even necessary to take quantum mechanical effects into account for an accurate description on the microscale. However, the computation of the behavior on a coarse length scale usually cannot be performed on a finer length scale due to computational limits. This shows the need of advanced analytical and numerical techniques to bridge the gap between the different scales.

One approach to overcome this problem is to derive a model on a coarse length scale from a model on a finer length scale. This process is called upscaling. Another approach is to couple models from different length scales into one multiscale model, see e.g. E and Engquist [6], Tadmor, Ortiz and Philips [17] and Wagner and Liu [19].

In this paper we focus on the relation between the atomistic and the continuum length scale. We use the inner expansion technique, which we proposed in [1], to derive a continuum model from an atomistic model for a crystalline solid. Our approach is based on an expansion of the macroscopic deformation function  $y$  and leads to a description of the potential energy in terms of the derivatives of  $y$  up to a given order. The incorporation of higher order gradients then allows for an accurate description of the material properties. In particular, it captures the discreteness effects from the atomistic model, in contrast to common continuum models. Thus we work within the quasi-continuum regime and have a well-defined and finite relation between the two length scales. This gives a better approximation than the thermodynamic limit process, which treats the atomistic scale as infinitesimally fine and assumes an infinite ratio of the two length scales.

At first glance, it seems useless to describe the discreteness effects by a continuum model, since the discrete atomistic model could be used directly instead. But this is not true. An advantage of the continuum model is that it is accessible to analytical techniques which allows to further investigate its properties. For the numerical treatment, the continuum mechanical model will be discretized again. This way, i.e. via the continuum model and its successive discretization, the original discrete atomistic model is transformed into another discrete model. The key point here is that the mesh size can be arbitrarily chosen, in contrast to the fixed number of atoms in the original atomistic system. Thus, the discretization error can be controlled. Moreover, it can be balanced with the model error which depends on the degree of approximation used in the derivation of the respective continuum mechanical system. Altogether, the computational accuracy can thus be adjusted to the desired accuracy of the solution. This permits an efficient implementation and makes it possible to simulate larger systems. It even allows for adaptive techniques, if necessary. In this respect the continuum model can serve as an averaging tool to pass from the atomistic discretization size to an arbitrary discretization size.

Higher order contributions in continuum mechanics have also been studied by Bar-

denhagen and Triantafyllidis [18]. Another technique to incorporate the discreteness of atomic systems into continuum mechanical models is the direct expansion technique, which is based on higher order gradients as well. It originates from Kruskal and Zabusky [13, 20] and has been further developed by Collins [4] and Rosenau [14, 15]. Numerical investigations for this approach have been performed by Kevrekidis et al. [12]. Furthermore, there is the so-called scaling technique, which passes to the continuum limit without taking the discreteness effects into account. It has been studied e.g. by Blanc, Le Bris and Lions [3] and E and Huang [7]. Finally, let us mention the work of Dreyer et al. [5] and Friesecke et al. [9, 10, 11] in the context of upscaling techniques. A comparison of different upscaling techniques is given in [1].

The remainder of this paper is organized as follows: In Section 3, a one-dimensional atomic chain with Hookean springs in the spirit of the famous work of Fermi, Pasta and Ulam [8] is considered. The inner expansion technique is applied to this chain and the qualitative and quantitative behavior of the technique is studied.

In Section 4, the inner expansion technique is applied to a realistic three-dimensional example, namely crystalline silicon. First, in Section 4.1, the quality of the approximation of the continuum energy is analyzed in the stationary setting. This is done for a system of moderate size, which allows a direct comparison with the atomistic system. From this, the optimal order of approximation can be obtained for a reasonable error tolerance. The results are then used in Section 4.2 to simulate the elastic behavior of the crystal for the corresponding evolution equation. The associated continuum system corresponds to an atomistic system of 12 billion atoms, which is impossible to be treated directly on the microscale with molecular dynamics techniques up to now.

## 2 INNER EXPANSION TECHNIQUE

### 2.1 Atomistic Potential

On the atomistic length scale, the specimen under consideration is described by a system of  $N$  atoms. Here we deal with crystalline solids, for which the atoms are arranged in form of a lattice  $\mathcal{L}$  in the reference configuration. The lattice is constructed from a base cell  $\mathcal{L}_{\text{cell}} \subset \mathbb{R}^d$ , which is nonempty and consists of a small, finite number of atoms. The lattice  $\mathcal{L}$  is then given by the infinite periodic continuation of  $\mathcal{L}_{\text{cell}}$  along the parallelepiped which is spanned by the column vectors of the regular matrix  $A \in \mathbb{R}^{d \times d}$ :

$$\mathcal{L} := \{x + Az \mid x \in \mathcal{L}_{\text{cell}}, z \in \mathbb{Z}^d\}. \quad (1)$$

The shape of the crystal is described by the bounded domain  $\Omega \subset \mathbb{R}^d$ . Hence the atoms of the specimen in the reference configuration are given by  $\mathcal{L} \cap \Omega$ . A deformation in space of the specimen is described by a function  $y : \mathcal{L} \cap \Omega \rightarrow \mathbb{R}^3$ . Thus the atom positions of the deformed specimen are given by  $\{y(x)\}_{x \in \mathcal{L} \cap \Omega}$ .

The behavior of the specimen is determined by the potential energy  $\Phi^{(A)}$ . Here the superscript (A) denotes the atomistic length scale. The potential energy is a function of

the atom positions  $y(x)$  for all  $x \in \mathcal{L}$ :

$$\Phi^{(A)} = \Phi^{(A)}(\{y(x)\}_{x \in \mathcal{L} \cap \Omega}). \quad (2)$$

We furthermore assume that the potential can be split into a sum of local interactions  $\Phi^{(A), \bar{x}}$  around some points  $\bar{x}$ :

$$\Phi^{(A)} = \sum_{\bar{x} \in \bar{\mathcal{L}} \cap \Omega} \Phi^{(A), \bar{x}}(\{y(x)\}_{x \in \mathcal{L} \cap \Omega}). \quad (3)$$

The points  $\bar{x}$  are chosen as the barycenter of the interaction. For example,  $\bar{x} = \frac{1}{2}(x + \tilde{x})$  if  $\Phi^{(A), \bar{x}}$  denotes the pair interaction of two atoms  $y(x)$  and  $y(\tilde{x})$ . Since the atom positions are arranged in form of a lattice, it makes sense to assume that this holds for the center points  $\bar{x}$  as well. Thus the set of center points  $\{\bar{x}\}$  forms the associated lattice  $\bar{\mathcal{L}} \cap \Omega$ . Note that  $\bar{\mathcal{L}}$  may, but need not coincide with  $\mathcal{L}$ .

The most simple example is the atomic chain in one dimension. To this end we consider the domain  $\Omega = (0, L)$  for some integer  $L > 0$  and place the atoms at the points  $1, 2, 3, \dots, L-2, L-1$ . The lattice is then given by  $\mathcal{L} = \mathbb{Z}$ . Adjacent atoms are connected by a spring of length 1 in the undeformed state. Furthermore we fix the chain at both ends, see Figure 1 for an illustration.



Figure 1: Atomic chain with fixed boundary.

The springs are assumed to obey Hooke's law with the spring constant normalized to 1. This gives rise to the potential

$$\Phi^{(A)}(\{y(x)\}_{x \in \mathcal{L} \cap \Omega}) = \sum_{x=1}^L \varphi(y(x) - y(x-1)) \quad \text{where} \quad \varphi(r) = \frac{1}{2}(r-1)^2. \quad (4)$$

To shorten notation, we assume  $y(x) = x$  for all lattice points outside  $\Omega$ . Note that these points only denote “fixed particles” without any degree of freedom and do not constitute particles of the system. In this way the specimen is subjected to the identity deformation at its boundary.

To obtain the localized formulation (3), we split (4) into its pair interactions. We then choose  $\bar{x}$  as the center point of each interacting particle pair and yield

$$\Phi^{(A)}(y) = \sum_{\bar{x} \in \bar{\mathcal{L}} \cap \Omega} \Phi^{(A), \bar{x}}(y), \quad \text{where} \quad \Phi^{(A), \bar{x}}(y) = \varphi\left(y\left(\bar{x} + \frac{1}{2}\right) - y\left(\bar{x} - \frac{1}{2}\right)\right) \quad (5)$$

with  $\bar{\mathcal{L}} = \mathbb{Z} + \frac{1}{2}$ .

## 2.2 Inner Expansion

So far we defined the potential energy  $\Phi^{(A)}$  on the atomistic level. Now we discuss its upscaling to the continuum mechanical level. There, the deformation function  $y$  is continuously defined on the whole domain  $\Omega \subset \mathbb{R}^d$ , not just discretely on the finite set  $\Omega \cap \mathcal{L}$  of atoms as for the atomistic level. Now, to such a deformation function  $y : \Omega \rightarrow \mathbb{R}^d$ , a potential energy has to be assigned.

To this end, we consider the Taylor expansion of  $y$  around some point  $\bar{x} \in \bar{\mathcal{L}} \cap \Omega$ . If  $y$  is sufficiently smooth, we have for  $x \in \Omega$ :

$$y(x) \approx \sum_{k=0}^K \frac{1}{k!} \nabla^k y(\bar{x}) : (x - \bar{x})^k. \quad (6)$$

Here  $K \in \mathbb{N}$  denotes the degree of approximation. The colon is a short notation for the higher dimensional scalar products. The expression (6) now allows us to rewrite the local potential  $\Phi^{(A),\bar{x}}$  as follows:

$$\begin{aligned} \Phi^{(A),\bar{x}}(\{y(x)\}_{x \in \mathcal{L} \cap \Omega}) &\approx \Phi^{(A),\bar{x}} \left( \left\{ \sum_{k=0}^K \frac{1}{k!} \nabla^k y(\bar{x}) : (x - \bar{x})^k \right\}_{x \in \mathcal{L} \cap \Omega} \right) \\ &= \Phi^{(I),\bar{x}}(y(\bar{x}), \nabla y(\bar{x}), \nabla^2 y(\bar{x}), \dots, \nabla^K y(\bar{x})). \end{aligned} \quad (7)$$

Here  $\Phi^{(I),\bar{x}}$  is defined by

$$\Phi^{(I),\bar{x}}(d_0, d_1, d_2, \dots, d_K) := \Phi^{(A),\bar{x}} \left( \left\{ \sum_{k=0}^K \frac{1}{k!} d_k : (x - \bar{x})^k \right\}_{x \in \mathcal{L} \cap \Omega} \right). \quad (8)$$

Thus we transformed the original potential  $\Phi^{(A),\bar{x}}$ , which depends on the deformation  $y$  at all lattice points  $x \in \mathcal{L} \cap \Omega$ , to a representation, which depends on the derivatives of  $y$ , evaluated only at the single point  $\bar{x}$ . Furthermore, according to (3), the overall potential  $\Phi^{(I)}$  is now given by

$$\Phi^{(I)}(y) = \sum_{\bar{x} \in \bar{\mathcal{L}} \cap \Omega} \Phi^{(I),\bar{x}}(y(\bar{x}), \nabla y(\bar{x}), \nabla^2 y(\bar{x}), \dots, \nabla^K y(\bar{x})). \quad (9)$$

## 2.3 Spatial averaging

The potential energy  $\Phi^{(I)}$  in representation (9) still contains the finite sum over all expansion points  $\bar{x} \in \bar{\mathcal{L}} \cap \Omega$ . This is in contrast to common continuum mechanical energies, in which an energy density is integrated over the reference configuration  $\Omega$ . The sum will now be approximated as follows: Observe that (9) is a Riemann sum, which is close to an integral. This justifies to interpolate it by passing to the integral representation

$$\Phi^{(J)}(y) = \frac{1}{|\det A|} \int_{\Omega} \Phi^{(I),\bar{x}}(y(\bar{x}), \nabla y(\bar{x}), \nabla^2 y(\bar{x}), \dots, \nabla^K y(\bar{x})) \, d\bar{x}. \quad (10)$$

The factor  $\frac{1}{|\det A|}$  stems from the volume of the base cell of the lattice, c.f. (1).

Here, the following remark is in order: Other upscaling techniques such as the scaling technique [3, 7] are based on the thermodynamic limit, which drives the number  $N$  of atoms to infinity. In this case the limiting procedure  $N \rightarrow \infty$  includes the limit of the Riemann sum and an integral representation is directly obtained. In contrast to this approach, the number  $N$  of atoms is kept fixed by the inner expansion technique. The passage from the Riemann sum to the integral representation is then an additional approximation step which does not correspond to the process of letting the number  $N$  of atoms tend to infinity. The result is not a description for the continuum limit, but an interpolated description for the system with a fixed number of atoms in the quasi-continuum regime, which still contains the discreteness effects of the finite system.

## 2.4 Evolution Equations

We are not only interested in the stationary potential but also in the time evolution of the system. For the atomistic system, this evolution is governed by Newton's second law of motion

$$m \frac{\partial^2 y(\tilde{x})}{\partial t^2} = -\nabla_{y(\tilde{x})} \Phi^{(A)}(\{y(x)\}_{x \in \mathcal{L} \cap \Omega}) \quad \forall \tilde{x} \in \mathcal{L} \cap \Omega, \quad (11)$$

where  $m$  denotes the mass of an atom. For the continuum mechanical system, it is given by

$$\rho \frac{\partial^2 y}{\partial t^2} = \sum_{k=0}^K (-1)^{k+1} \operatorname{div}^k \Phi_{,k}^{(1),x}(y, \nabla y, \nabla^2 y, \dots, \nabla^K y) \quad \text{in } \Omega, \quad (12)$$

where  $\Phi_{,k}^{(1),x}$  denotes the derivative of  $\Phi^{(1),x}$  with respect to the variable  $\nabla^k y$  and  $\rho = |\det A|^{-1} m$  is the mass density. This equation is derived by applying Newton's law for a test function  $v \in C_c^\infty(\Omega)$  to the overall potential  $\Phi^{(J)}(y)$  as given by (10). This reads as  $\int_\Omega \rho \frac{\partial^2 y}{\partial t^2} v = -\Phi^{(J)'}(y; v)$ , where  $\Phi^{(J)'}(y; v)$  denotes the derivative of  $\Phi^{(J)}$  at  $y$  in direction  $v$ . Integration by parts and passing to the pointwise formulation then leads to (12).

## 3 NUMERICAL EXAMPLE: ATOMIC CHAIN

As a first example, we consider the atomic chain as given in Section 2. Despite of its simplicity, it can serve quite well as a model problem. Many effects from realistic problems can already be studied here.

The inner expansion of the spring potential as given by (5) now reads as

$$\begin{aligned} \Phi^{(1),\bar{x}}(d_0, d_1, d_2, \dots, d_K) &= \Phi^{(A),\bar{x}} \left( \left\{ \sum_{k=0}^K \frac{1}{k!} d_k : (x - \bar{x})^k \right\}_{x \in \mathcal{L} \cap \Omega} \right) \\ &= \varphi \left( \sum_{k=0}^K \frac{1}{k!} d_k : \left( \bar{x} + \frac{1}{2} - \bar{x} \right)^k - \sum_{k=0}^K \frac{1}{k!} d_k : \left( \bar{x} - \frac{1}{2} - \bar{x} \right)^k \right) \end{aligned}$$

$$= \varphi \left( \sum_{k=1 \dots K, k \text{ odd}} \frac{2^{1-k}}{k!} d_k \right), \quad (13)$$

where  $\varphi$  denotes the specific pair potential function from (4). Thus, the interpolated quasi-continuum energy  $\Phi^{(J)}$  is given by

$$\Phi^{(J)}(y) = \frac{1}{2} \int_{\Omega} y'^2(x) \, dx \quad \text{for } K = 1, 2, \quad (14)$$

$$\Phi^{(J)}(y) = \frac{1}{2} \int_{\Omega} \left( y'(x) + \frac{1}{24} y'''(x) \right)^2 \, dx \quad \text{for } K = 3, 4. \quad (15)$$

According to (12), the macroscopic evolution equation then reads as

$$\frac{\partial^2 y}{\partial t^2} = \frac{\partial^2 y}{\partial x^2} \quad \text{for } K = 1, 2, \quad (16)$$

$$\frac{\partial^2 y}{\partial t^2} = \frac{\partial^2 y}{\partial x^2} + \frac{1}{12} \frac{\partial^4 y}{\partial x^4} + \frac{1}{576} \frac{\partial^6 y}{\partial x^6} \quad \text{for } K = 3, 4. \quad (17)$$

Relation (16) is the well-known linear wave equation, while (17) contains additional terms which stem from the discreteness of the system.

The continuum mechanical model is augmented by the boundary conditions

$$y(x, t) = x \quad \forall x \in \partial\Omega \quad \text{for } K = 1, 2, \quad (18)$$

$$y(x, t) = x, \quad \frac{\partial y}{\partial x}(x, t) = 1, \quad \frac{\partial^2 y}{\partial x^2}(x, t) = 0 \quad \forall x \in \partial\Omega \quad \text{for } K = 3, 4 \quad (19)$$

for all  $t \geq 0$ . They stem from the fixation of the atomic chain at its boundary, which states that the chain is embedded in an infinite undeformed chain. This implies for the continuum model that  $y$  and its derivatives coincide with the identity deformation and its derivatives at the boundary.

Note finally that for larger  $K$  equations and boundary conditions analogous to (16, 17) and (18, 19) can be derived which involve higher order derivative terms.

Altogether, for the specific choices of  $K = 1, \dots, 4$ , we have macroscopic quasi-continuum models at our disposal. Now we will discretize these equations and solve them numerically. To this end, we employ suitable finite differences in space and time. For the time discretization, an explicit scheme with a three-point stencil is sufficient. The time step-size is chosen small enough to satisfy the CFL condition. This ensures the stability of the scheme. For the spatial discretization, the divergence structure of the PDE is exploited by a two stage scheme. In the first step, the derivatives  $\Phi_{,k}^{(J),x}$  are computed. In the second step, the divergence operators are applied.

In both steps, a high order difference stencil is necessary to resolve the spatial derivatives. A stencil which is consistent only up to order 1 or 2 introduces a considerable

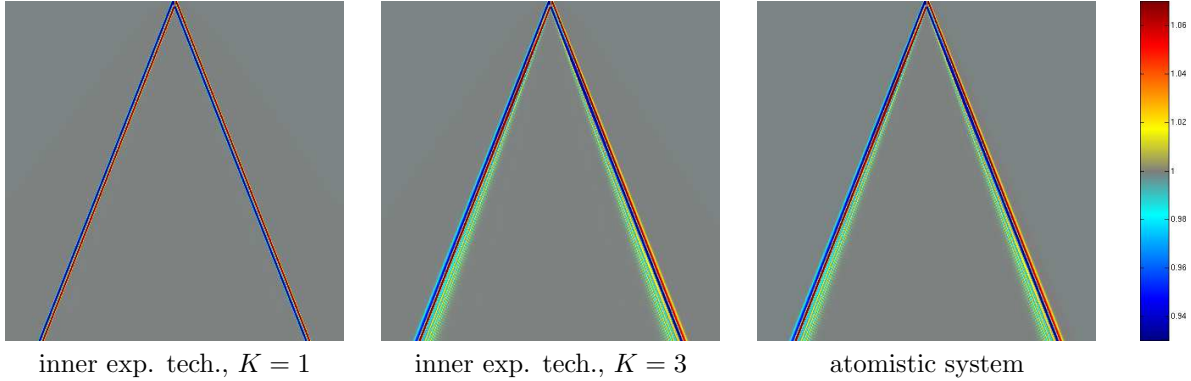


Figure 2: Atomic chain: Solution of (16), (17) and the underlying atomistic system.

amount of higher order error terms, which interfere with the terms that involve higher order derivatives which resemble the discreteness of the atomistic system. Since we are interested in the discreteness effects of the PDE and not in the consistency error of the finite difference stencils, we cannot use such low order stencils but have to use stencils with sufficiently high order instead. Therefore, in all numerical examples given below, 10-point stencils are used in both steps. They possess a consistency order of 10 minus the order of the derivative under consideration. This results in a consistency order of at least six in the applications studied below. Now the spatial discretization errors of low order are eliminated and basically all visible dispersion comes from the PDE itself.

In the following we present the results of our numerical calculations. Here, the domain is given by  $\Omega = (0, 1000)$ . This corresponds to a chain of 999 atoms with lattice constant 1. The initial values at time  $t = 0$  are given by  $y(x, 0) = x + p(x)$  and by  $\frac{\partial y}{\partial t}(x, 0) = 0$  for all  $x \in \Omega$ . The function  $p \in C^3([0, 1000])$  denotes a small perturbation around the center  $x = 500$ . It is a piecewise 7th-order polynomial such that  $p \equiv 0$  on  $[0, 490] \cup [510, 1000]$ ,  $p(500) = 1$  and  $p'(x) = p''(x) = p'''(x) = 0$  for  $x = 490, 500, 510$ .

The solutions of (16) and (17) after discretization are shown in Figure 2. The  $x$ -axis is plotted horizontally and the  $t$ -axis vertically from top to bottom. The color indicates the quantity  $(y')^{-1}$ , which corresponds to the atom density of the atomistic model. Gray denotes regions with the equilibrium density 1, yellow and red regions with a higher density and blue regions with a lower density, compare the color-bar. Additionally the solution of the underlying atomistic system is depicted as reference.

One can clearly observe the propagation of the initial perturbation with constant speed to the left and to the right side. The propagation speed is reproduced correctly in both continuum models. For  $K = 1, 2$ , the initial perturbation is propagated without changing its shape. This is in full agreement with the established theory for the linear wave equation (16). But this behavior does not match that of the original atomistic system for which a distinct amount of dispersion due to the discreteness of the underlying atomistic system can be observed. This dispersion, however, is captured by the continuum model for  $K = 3, 4$ . Its solution coincides very well with the solution of the original atomistic

system. The dispersion is reproduced both qualitatively and quantitatively to a high extent.

We also tested our new technique for  $K \geq 5$ , which leads to quasi-continuum models involving additional terms with higher derivatives than that in (17). The resulting solutions (of course we then used finite difference stencils of appropriate higher order) did not show any noticeable difference from that of (17). Thus, the expansion technique with  $K = 3$  already gives a very good quasi-continuum approximation of the model. The involved terms up to the 6th order derivative suffice to accurately describe the microscopic effects.

## 4 NUMERICAL EXAMPLE: SILICON CRYSTAL

So far, we introduced the inner expansion technique and studied it for a simple one-dimensional model problem. We now apply it to a more realistic problem in three dimensions, namely to crystalline silicon.

### 4.1 Approximation of potential energy

A widely used potential for the atomistic simulation of silicon has been given by Stillinger and Weber [16]. It consists of two-body and three-body interactions and reads

$$\begin{aligned} \Phi^{(A)}(\{y(x)\}_{x \in \mathcal{L} \cap \Omega}) &= \frac{1}{2} \sum_{x_1, x_2} \varphi_2(|y(x_2) - y(x_1)|) \\ &+ \frac{1}{2} \sum_{x_1, x_2, x_3} \varphi_3 \left( |y(x_2) - y(x_1)|, |y(x_3) - y(x_1)|, \frac{(y(x_2) - y(x_1)) \cdot (y(x_3) - y(x_1))}{|y(x_2) - y(x_1)||y(x_3) - y(x_1)|} \right). \end{aligned} \quad (20)$$

The two-body interactions

$$\varphi_2(r) = \varepsilon A \left( B \frac{\sigma^4}{r^4} - 1 \right) \exp \frac{\sigma}{r - \sigma a} \quad (21)$$

stabilize the equilibrium distance of two adjacent atoms in the lattice. Here, the exponential term serves as a cutoff function. The three-body interactions

$$\varphi_3(r_{12}, r_{13}, \Theta) = \varepsilon \lambda \exp \left( \frac{\gamma \sigma}{r_{12} - \sigma a} + \frac{\gamma \sigma}{r_{13} - \sigma a} \right) \left( \Theta + \frac{1}{3} \right)^2 \quad (22)$$

depend on the angle  $\Theta$  between  $y(x_2) - y(x_1)$  and  $y(x_3) - y(x_1)$  and again contain a cutoff function. They favor the angle  $\arccos(-\frac{1}{3}) \approx 109.47^\circ$ . Together, these two- and three-body interactions result in an overall potential energy which is minimal just if the atoms are arranged in the so-called diamond lattice structure. This is the natural lattice structure of silicon. The involved material constants are given by  $A = 7.049556277$ ,

$B = 0.6022245584$ ,  $\lambda = 21.0$ ,  $\gamma = 1.2$ ,  $\sigma = 0.20951\text{nm}$ ,  $\varepsilon = 50\text{kcal/mol}$  and  $a = 1.8$ , see [16].

We now apply our inner expansion technique in a straightforward but tedious calculation to the potential of Stillinger and Weber. To this end,  $\Phi^{(A)}$  is localized by splitting it up into all two-body and three-body interactions. The different interaction terms are expanded by a Taylor series up to order  $K$ . The expansion points  $\bar{x}$  are chosen as  $\bar{x} = \frac{1}{2}(x_1 + x_2)$  and  $\bar{x} = \frac{1}{3}(x_1 + x_2 + x_3)$ , respectively. Then, the potential is rewritten in terms of the derivatives of  $y$  as in (9). Finally, we interpolate the potential as described in Section 2.3 and obtain the associated integral formulation (10).

Now an appropriate order  $K$  of approximation has to be determined. To this end, we compute the potential energy of a non-trivially deformed specimen for different values of  $K$  and compare it to the value of the original atomistic system. The reference configuration of the specimen is a cube which consists of 32768 atoms. The two opposite faces of the cube perpendicular to the  $x_1$ -axis are displaced by a shearing with a ratio  $\delta$  ranging from 0 to 0.2. The specimen in-between is smoothly interpolated by

$$q(x_1, x_2, x_3) = (x_1, x_2 + p(x_1), x_3). \quad (23)$$

Here  $p$  denotes the fifth-order polynomial such that  $p(0) = 0$ ,  $p(L) = \delta$  and  $p'(0) = p''(0) = p'(L) = p''(L) = 0$  where  $L$  is the length of the cube edges.

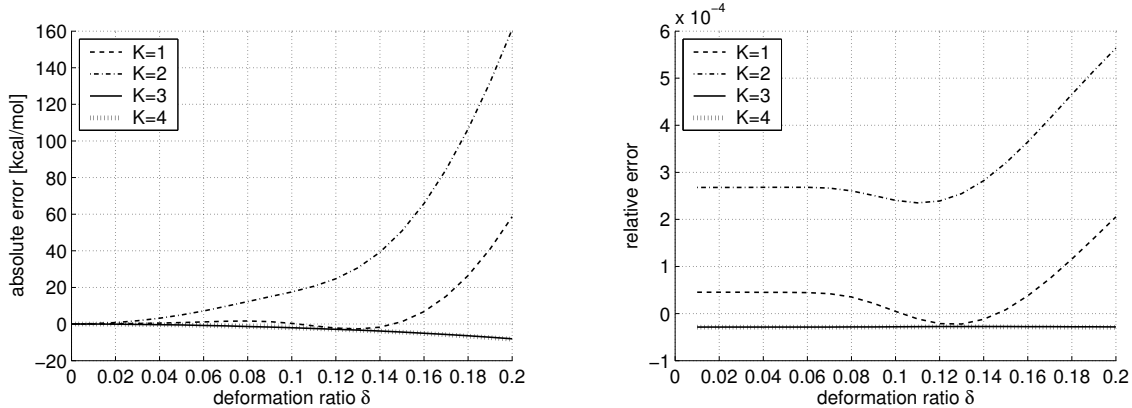


Figure 3: Absolute and relative error of the Stillinger-Weber potential for the inner expansion technique with  $K = 1, 2, 3, 4$ .

Figure 3 shows the result of the comparison for different deformation ratios and for  $K = 1, 2, 3, 4$ . The left plot shows the absolute error with respect to the atomistic system as the reference solution. The right plot shows the relative error. For  $K = 1$ , it stays below 0.2% for the considered range of deformation, which is already quite good. For  $K = 2$ , the error is larger, but still remains below 0.6%. For  $K = 3$ , the error is even below 0.03%. The values for  $K = 3$  and  $K = 4$  nearly coincide. Thus it does not make

any sense to use  $K = 4$  instead of  $K = 3$ . For  $K = 1$  and  $K = 2$ , the error strongly depends on the deformation ratio, whereas it is nearly constant for  $K = 3$  and  $K = 4$ . All in all, the value of  $K = 3$  seems to be sufficient for this type of potential.

Let us note that the influence of the higher order contributions depends on the size of the system. It gets successively smaller for an increasing number of atoms. Thus for systems with a very high number of atoms, it might even be appropriate to use  $K = 1$ , since the higher order contributions are negligibly small then. But they result in a qualitatively different behavior in the evolution equation as we have seen already in Section 3. Thus it might be justified to incorporate them despite their quantitatively small contribution to the overall energy.

## 4.2 Dynamics of elastic behavior

Now we consider the time evolution of a silicon crystal, which is governed by equation (12). We are interested in the elastic response of the crystal. To this end, we choose as initial value the deformation  $q$  as given by (23) with the deformation ratio  $\delta = 0.1$ , together with an initial velocity of zero. The boundary values are chosen in such a way that the specimen is embedded into an infinite bulk crystal which underwent the same deformation. Analogously to (19), this reads as

$$y(x) = q(x), \quad \nabla_\nu y(x) = \nabla_\nu q(x), \quad \nabla_\nu^2 y(x) = \nabla_\nu^2 q(x) \quad \forall x \in \partial\Omega. \quad (24)$$

According to the considerations in the previous section, we use  $K = 3$ . The spatial discretization is done by finite differences where we exploit the divergence structure of the PDE as in the last section. Now, in the three-dimensional setting, this is even more important, since it considerably reduces the computational costs. In a first step, the discrete derivatives up to order 3 are computed. Then, in a second step, the discrete divergence operators are applied. For both steps, a tensor product difference stencil of one-dimensional 5-point stencils is used. The stencils are consistent of order 4 for the first and second derivative and of order 2 for the third derivative. This ensures a sufficient accuracy. For the time discretization, an explicit Euler scheme is used.

The dimensions are chosen such that, after the finite difference discretization of the continuum mechanical system, each grid point corresponds to  $64^3 = 262.144$  atoms. We use  $36^3 = 46.656$  grid points, hence the complete continuum system models 12.230.590.464 atoms. For the time-step, a value of 0.2ps turned out to be sufficient. This is substantially larger than the time-step size of 1fs which is usually needed for atomistic simulations.

Figure 4 shows the results of the simulation at different time-steps. The plots show a planar cross section through the specimen. The associated displacement of the specimen is visualized using a mesh. It is magnified by a factor of 8 for better visibility. The color furthermore indicates the velocity in the  $x_1$ -direction.

One can clearly observe that the system tends to relax from the initial configuration. The relaxation leads to the natural oscillations of the specimen. First one can observe

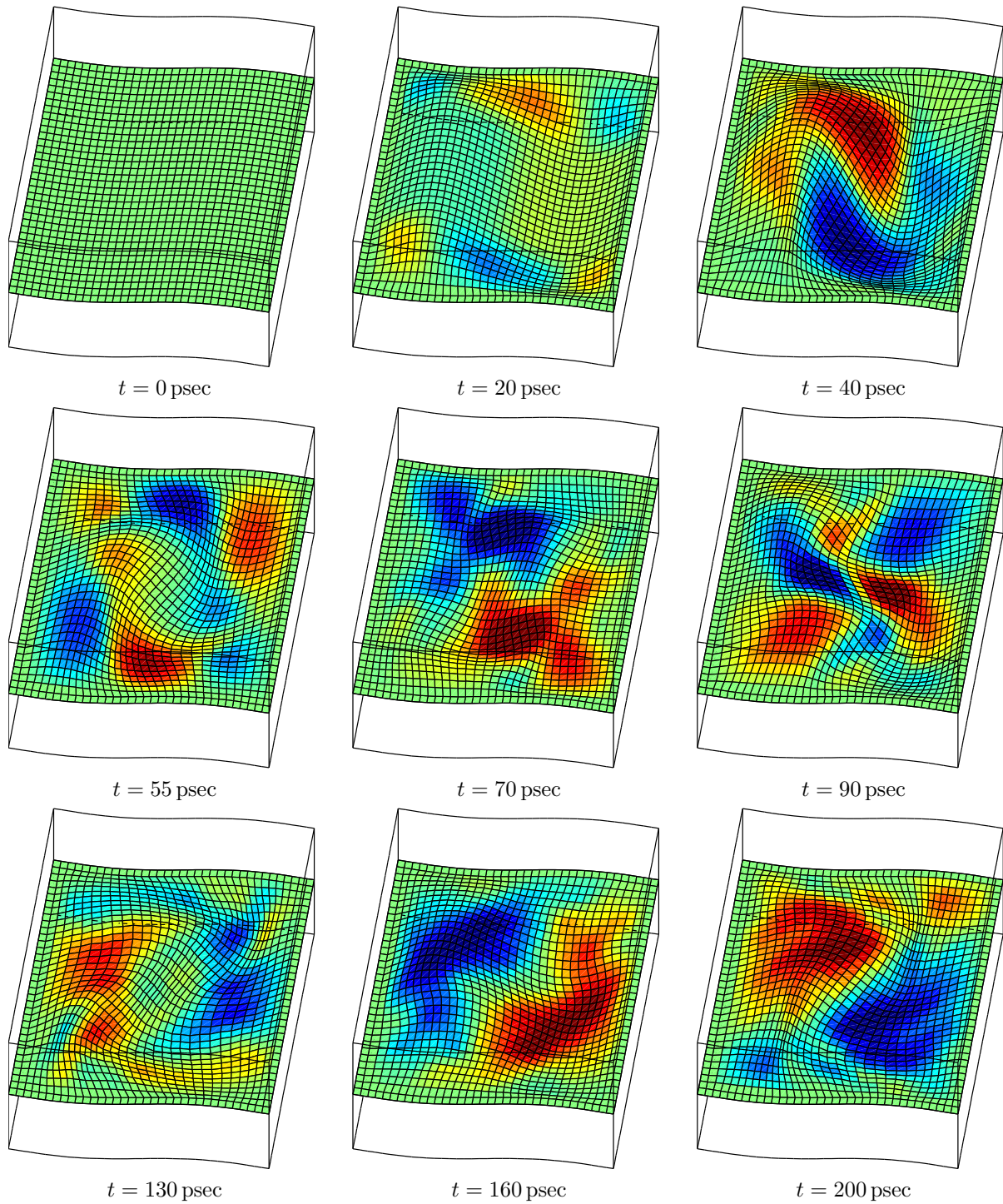


Figure 4: Elastic behavior of silicon. The cross-section shows the displacement, magnified by the factor 8. The color denotes the velocity in  $x_1$ -direction (plotted horizontally).

basically a circular movement of the whole inner part of the specimen. Later on additional local oscillations with a higher frequency develop.

## 5 CONCLUSION

We proposed the inner expansion technique to derive quasi-continuum models from atomistic systems for crystalline solids. This approach is capable to capture the associated material properties to a high extent, including those due to nonlinear deformations such as bending. Furthermore the discreteness effects of the underlying atomistic model are reproduced correctly, in contrast to classical continuum limits. We showed this numerically for the simple model problem of an atomic chain. Furthermore we applied the technique to a silicon crystal and presented a numerical simulation of the time evolution of its elastic response.

The main advantages of the quasi-continuum model compared to the atomistic model are as follows: Its numerical solution is much less costly, because the resolution of the discretization can be freely controlled, whereas the already discrete atomistic model is restricted to the physically given discreteness. This allows to use quite coarse grids for the discretization of the homogenized macroscopic model without losing its atomistic discreteness properties. Furthermore, much larger time step sizes than on the atomistic scale can be used. Moreover, advanced numerical techniques like adaptivity can be applied if necessary and also analytical techniques for PDEs might be used. Finally, the rigorously derived higher order terms can be a good starting point to formulate improved phenomenological models. These models still coincide with the correct ones to a good extent, but might be easier to handle. For an application involving such higher order terms in the context of shape memory alloys, see e.g. [2].

Classical continuum mechanics deals with systems in the order of  $10^{23}$  atoms for which the classical continuum limit often is a good description. But the advances in nanotechnology in the last years make it necessary to consider systems with a substantially smaller size of atoms for which the full continuum description clearly fails. On the other hand, these systems are still not in the reach of conventional molecular dynamics methods due to complexity reasons and the necessary involved small time step sizes. In this respect a quasi-continuum approach gets more and more important also for practical applications. Here, a well-understood transition from the atomistic level to the quasi-continuum level is essential for further developments towards multiscale simulations, bridging techniques and similar approaches involving models on different scales, see e.g. [17] and [19].

**REFERENCES**

- [1] M. Arndt and M. Griebel. Derivation of higher order gradient continuum models from atomistic models for crystalline solids. *Multiscale Model. Simul.*, 2004. Submitted.
- [2] M. Arndt, M. Griebel, and T. Roubíček. Modelling and numerical simulation of martensitic transformation in shape memory alloys. *Contin. Mech. Thermodyn.*, 15(5):463–485, 2003.
- [3] X. Blanc, C. Le Bris, and P.-L. Lions. From molecular models to continuum mechanics. *Arch. Ration. Mech. Anal.*, 164(4):341–381, 2002.
- [4] M. A. Collins. A quasicontinuum approximation for solitons in an atomic chain. *Chem. Phys. Lett.*, 77(2):342–347, 1981.
- [5] W. Dreyer and R. Guckel. Micro-macro transitions by interpolation, smoothing/averaging and scaling of particle trajectories. Preprint No. 725, WIAS Berlin, 2002.
- [6] W. E and B. Engquist. The heterogeneous multi-scale methods. *Comm. Math. Sci.*, 1(1):87–133, 2003.
- [7] W. E and Z. Huang. A dynamic atomistic-continuum method for the simulation of crystalline materials. *J. Comput. Phys.*, 182(1):234–261, 2002.
- [8] E. Fermi, J. Pasta, and S. Ulam. Studies of nonlinear problems I. Report LA-1940, Los Alamos Scientific Laboratory, 1955. Reprinted in: *Nonlinear Wave Motion*, A. C. Newell (ed.), AMS Lect. Appl. Math. 15:143–156, 1974.
- [9] G. Friesecke and R. D. James. A scheme for the passage from atomic to continuum theory for thin films, nanotubes and nanorods. *J. Mech. Phys. Solids*, 48(6–7):1519–1540, 2000.
- [10] G. Friesecke and R. L. Pego. Solitary waves on FPU lattices: I. qualitative properties, renormalization and continuum limit. *Nonlinearity*, 12(6):1601–1627, 1999.
- [11] G. Friesecke and F. Theil. Validity and failure of the Cauchy-Born hypothesis in a two-dimensional mass-spring lattice. *J. Nonlinear Sci.*, 12(5):445–478, 2002.
- [12] P. G. Kevrekidis, I. G. Kevrekidis, A. R. Bishop, and E. S. Titi. Continuum approach to discreteness. *Phys. Rev. E*, 65(4):046613, 2002.
- [13] M. D. Kruskal and N. J. Zabusky. Stroboscopic perturbation procedure for treating a class of nonlinear wave equations. *J. Math. Phys.*, 5(2):231–244, 1964.
- [14] P. Rosenau. Dynamics of dense lattices. *Phys. Rev. B*, 36(11):5868–5876, 1987.

- [15] P. Rosenau. Hamiltonian dynamics of dense chains and lattices: or how to correct the continuum. *Phys. Lett. A*, 311(1):39–52, 2003.
- [16] F. H. Stillinger and T. A. Weber. Computer simulation of local order in condensed phases of silicon. *Phys. Rev. B*, 31(8):5262–5271, 1985.
- [17] E. B. Tadmor, M. Ortiz, and R. Phillips. Quasicontinuum analysis of defects in solids. *Philos. Mag. A*, 73(6):1529–1563, 1996.
- [18] N. Triantafyllidis and S. Bardenhagen. On higher order gradient continuum theories in 1-D nonlinear elasticity. Derivation from and comparison to the corresponding discrete models. *J. Elasticity*, 33(3):259–293, 1993.
- [19] G. J. Wagner and W. K. Liu. Coupling of atomistic and continuum simulations using a bridging scale decomposition. *J. Comput. Phys.*, 190(1):249–274, 2003.
- [20] N. J. Zabusky and M. D. Kruskal. Interaction of "solitons" in a collisionless plasma and the recurrence of initial states. *Phys. Rev. Lett.*, 15(6):240–243, 1965.